ISSN 0021-3640, JETP Letters, 2014, Vol. 99, No. 7, pp. 405–409. © Pleiades Publishing, Ltd., 2014.
Original Russian Text © S.M. Zharkov, E.T. Moiseenko, R.R. Altunin, N.S. Nikolaeva, V.S. Zhigalov, V.G. Myagkov, 2014, published in Pis'ma v Zhurnal Eksperimental'noi i Teoreticheskoi Fiziki, 2014, Vol. 99, No. 7, pp. 472–477.

Study of Solid-State Reactions and Order–Disorder Transitions in Pd/α-Fe(001) Thin Films

S. M. Zharkov[a, b], E. T. Moiseenko[a, b], R. R. Altunin[a, b], N. S. Nikolaeva[b], V. S. Zhigalov[a, c], and V. G. Myagkov[a]

[a] *Kirensky Institute of Physics, Siberian Branch, Russian Academy of Sciences, Krasnoyarsk, 660036 Russia*
e-mail: zharkov@iph.krasn.ru
[b] *Siberian Federal University, Krasnoyarsk, 660041 Russia*
[c] *Siberian State Aerospace University, Krasnoyarsk, 660014 Russia*

Received February 28, 2014; in final form, March 11, 2014

The formation of the hard-magnetic ordered $L1_0$–FePd phase in thin bilayer Pd/α-Fe(001) films has been experimentally studied. Solid-state reactions initiated by thermal heating in bilayer Pd/α-Fe(001) films with a thickness of 50–60 nm (the atomic ratio Pd : Fe ≈ 50 : 50) separated from the substrate have been studied using the in situ electron diffraction methods. It has been shown that the solid-state reaction between the palladium and iron layers in Pd/α-Fe(001) starts at 400°C with the formation of the disordered Fe–Pd phase. At 480°C, the ordered $L1_0$–FePd phase is formed. The order–disorder phase transition has been studied. It has been established that the transition of the ordered $L1_0$–FePd phase to the disordered FePd phase starts at 725°C. At 740°C, only the disordered FePd phase is present over the whole volume of the film. The observed temperature of the order–disorder phase transition is shifted from the equilibrium value by 35°C to higher temperatures. This effect is assumingly associated with the higher concentration of palladium atoms at the boundaries of the Fe–Pd crystal grains owing to the grain-boundary adsorption.

DOI: 10.1134/S0021364014070145

Nanomaterials on the basis of FePd, FePt, and CoPt with the ordered structure of the $L1_0$ type are of high fundamental and applied interest owing to the possibility of their application as a material for superdense magnetic recording [1–5]. Such materials have unique magnetic properties: a large coercive force ($H_c > 1.0$ kOe) and a high uniaxial magnetic anisotropy ($K_u \sim 10^7$–10^8 erg/cm^3), which is due to the tetragonal symmetry of the crystal structure of the $L1_0$ phase.

In [6], the initial stage of the solid-state reaction and the formation of the ordered $L1_0$ phase in thin bilayer single-crystal Fe(101)/Pd(001) films was studied. Films were prepared in high vacuum by the subsequent deposition of 5-nm Pd and 5-nm Fe on a MgO(001) substrate heated to 350°C. It was found that fast intermixing starts between the Fe and Pd layers at a temperature of 400°C and the $L1_0$ phase is simultaneously formed.

In [7], the formation of the $L1_0$–FePd phase in the multilayer films [Fe(2.50 nm)/Pd(0.75–5.50 nm)]$_8$ was studied. The prepared films were annealed in vacuum for 1 h at a fixed temperature in the temperature range of 300–700°C. It was shown that, in the process of annealing of films at the Pd layer thickness of 3.00–3.50 nm, the fcc Fe and Pd phases present in the film in the initial state are transformed into the $L1_0$–FePd phase at an annealing temperature above 400°C.

In [8], when studying the process of the transition from the structurally disordered FePd phase to the ordered $L1_0$–FePd phase, the formation of the intermediate disordered phase of the A6 type (body-centered tetragonal structure, the space group $I4/mmm$) was observed. The studies were performed on FePd single crystals with the disordered structure. The intermediate phase was observed after annealing of samples at 500–600°C for several hours.

Experimental results of studying the solid-state synthesis of the $L1_0$–FePd phase in the epitaxial film system Fe(001)/Pd(001) grown on the MgO(001) substrate were presented in [9, 10]. The formation of the structure consisting of crystallites of the ordered $L1_0$ phase with the c axes coinciding with three directions [100], [010], and [001] of the MgO(001) substrate was observed at an annealing temperature of 450°C.

The analysis of the published data indicates that studies of the solid-state reactions and the formation of the ordered structures in the film system Fe–Pd, as a rule, are performed on film systems located directly on the substrate. Either the initial stage of the solid-state reactions between Fe and Pd layers or the process of the atomic ordering in the already formed structurally disordered FePd phase is under study.

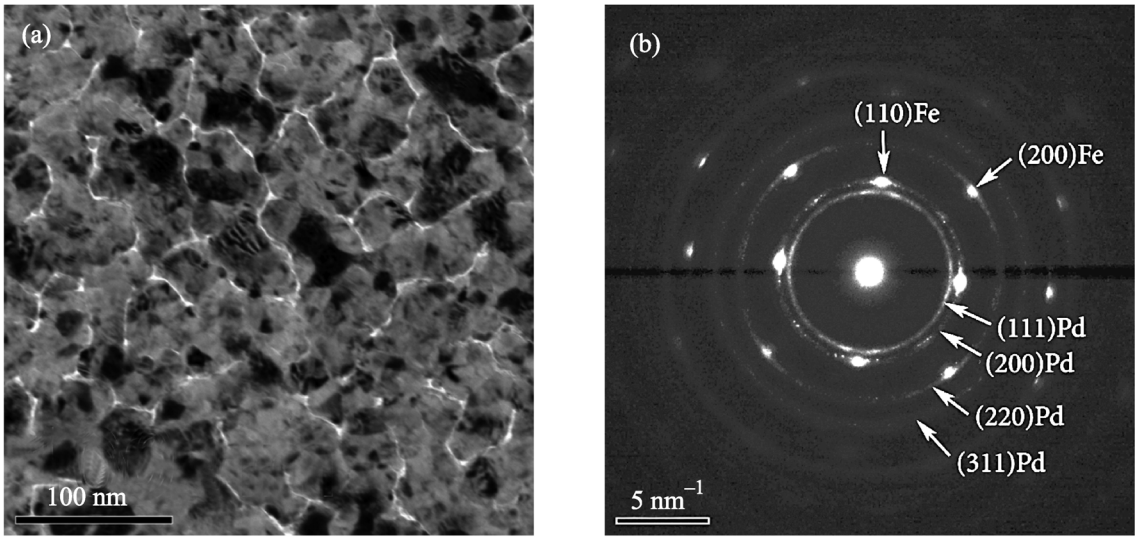

Fig. 1. (a) Transmission electron microscopy image and (b) electron diffraction pattern of the Pd/α-Fe(001) film in the initial state.

This work was aimed at the in situ study of the phase transitions during thermal heating in thin bilayer Pd/α-Fe(001) films separated from the substrate. The study of the formation of the hard-magnetic ordered $L1_0$–FePd phase and its temperature stability and the possibility of the formation of intermediate phases is of particular interest.

Bilayer thin Pd/α-Fe(001) films studied in this work were prepared by successive deposition of Fe and Pd layers on the substrate by means of high-vacuum thermal evaporation (the base vacuum of 10^{-4} Pa). Freshly cleaved NaCl(001) single crystals were used as the substrate. The substrate temperature during deposition of the first layer (Fe) was 220–250°C in order to obtain the epitaxial α-Fe(001) film on NaCl(001). The substrate was at room temperature when the second layer (Pd) was deposited. The total thickness of the bilayer Pd/Fe film was 50–60 nm. The ratio of the individual thicknesses of the Fe and Pd layers was chosen so that the Pd content was about 50 at %. According to the phase equilibrium diagram [11], the stability region of the FePd phase is in the range of 50.0–60.5 at % Pd. The microstructure and phase and element compositions of the Pd/Fe films were studied using transmission electron microscopy, electron diffraction, and energy dispersive spectroscopy on a JEM-2100 transmission electron microscope (JEOL) equipped with an Inca x-sight energy dispersive spectrometer (Oxford) [12–14]. The element analysis showed that the atomic ratio Pd : Fe in the studied samples was about 50 : 50.

The Pd/Fe films were heated directly in the column of the JEM-2100 transmission electron microscope (JEOL) using a sample holder with an option of the controlled heating from room temperature to 1000°C (Gatan Model 652 Double Tilt Heating Holder). To this end, the Pd/Fe films were separated from the substrate and were placed on the electron-microscope supporting molybdenum grids. Recording of electron diffraction patterns (at a speed of 4 fpm) and synchronous sample temperature measurement were performed simultaneously with heating. The diffraction patterns were identified using the program DigitalMicrograph (Gatan) and crystal structure databases: ICDD PDF 4+ [15] and Pearson's Databases [16].

A transmission electron microscopy image of Pd/Fe films in the initial state is shown in Fig. 1a. The analysis of the diffraction reflections in the electron diffraction pattern (Fig. 1b) indicates that the following phases are present in the film: α-Fe with the bcc lattice and the space group Im-3m with the lattice parameter $a = 2.866$ Å (PDF 4+ card 00-006-0696), Pd with the fcc lattice and the space group Fm-3m with the lattice parameter $a = 3.890$ Å (PDF 4+ card 00-046-1043), and Fe_3O_4 with the spinel structure and the space group Fd-3m with the lattice parameter $a = 8.396$ Å (PDF 4+ card 04-005-4319).

The main part of the spot diffraction reflections (Fig. 1b) correspond to the single-crystal α-Fe phase with the orientation (001), which consists of coherently oriented α-Fe crystallites. High stresses arise in the thin film in the process of the epitaxial growth [17]. As a result, the separation into individual crystallites takes place, which is observed in the transmission electron microscopy image (Fig. 1a).

Spot reflections ($d \approx 3.0$ Å) with the intensity <1% are also observed in the diffraction pattern (Fig. 1b). These reflections correspond to the Fe_3O_4 phase $d(220) = 2.97$ Å with the orientation relation $Fe_3O_4(001)[110] \parallel$ α-Fe(001)[001]. The formation of the Fe_3O_4 phase is associated with the surface oxida-

tion of the external side of the Fe layer in the process of the separation of the film from the substrate. The analysis of the intensity of reflections of the Fe_3O_4 phase makes it possible to assume that the effective thickness of the oxide layer is 1–2 nm. The analysis of the element composition of the Pd/Fe films in the initial state showed the presence of oxygen ≈20 at %. It is possible to assume that a small part of oxygen enters iron oxide formed as centers of nucleation on the crystalline defects of iron grains, and the main part is oxygen adsorbed on the surface of the Fe film.

The main part of the polycrystalline diffraction reflections (Fig. 1b) corresponds to the Pd phase with the crystallite size of ≈20–40 nm. In the diffraction rings, a texture is observed that indicates the presence of a small part of Pd in the film with the preferred orientation of crystallites corresponding to the orientation relation α-Fe (001)[110] || Pd(001)[001]. The same orientation relation was found during the epitaxial growth of α-Fe and Pd layers [8].

Thus, the main part of the sample in the initial state is the thin-film system Pd/α-Fe(001)/Fe_3O_4(001): the first layer (25–30 nm thick) is Pd with the polycrystalline structure, the second layer (25–30 nm thick) is α-Fe with the single-crystal structure with the orientation (001), and the third layer (the effective thickness of 1–2 nm) is Fe_3O_4 with the single-crystal structure with the orientation (001).

The change in the phase composition of the films Pd/α-Fe(001) during heating was studied by in situ electron diffraction. Samples were heated from room temperature to 700°C with subsequent annealing. The heating rate was 8°C/min. The first signs of the solid-state reaction were recorded when a temperature of 305°C was reached. Weak spot diffraction reflections with a relative intensity of 1% corresponding to an interplanar distance of Fe_3O_4 $d(440) = 1.48$ Å appeared in the electron diffraction pattern. The intensity of these reflections remained almost the same to 405°C. Their intensity increased only at the further increase in the temperature. At 535°C, the intensity of the spot reflections $d(220) = 2.97$ Å and $d(440) = 1.48$ Å of Fe_3O_4 reaches 5–10%. Then, it starts to decrease. At 550°C, the reflections of Fe_3O_4 are no longer observed. Apparently, with increasing temperature above 400°C, the centers of nucleation of the iron oxide phase coalesce, leading to the increase in the average size of Fe_3O_4 particles. This is confirmed indirectly by the increase in the intensity of the diffraction reflections in the electron diffraction patterns. With temperature increasing to 550°C, the thermal decomposition of Fe_3O_4 takes place and adsorbed oxygen is removed from the surface. The results obtained in this work are in agreement with [7], where it was shown that a phase interpreted as Fe_2O_3 was formed in the multilayer films $[Fe(2.5\ nm)/Pd(3.0–3.5\ nm)]_8$ subjected to high-vacuum annealing at a temperature of 350°C. This phase was also observed in films with thinner Pd (3.0 nm) layers after annealing at 550°C. In films with a Pd thickness of 3.5 nm, no reflections corresponding to the iron oxide phase are observed in the electron diffraction pattern after annealing at 550°C [7].

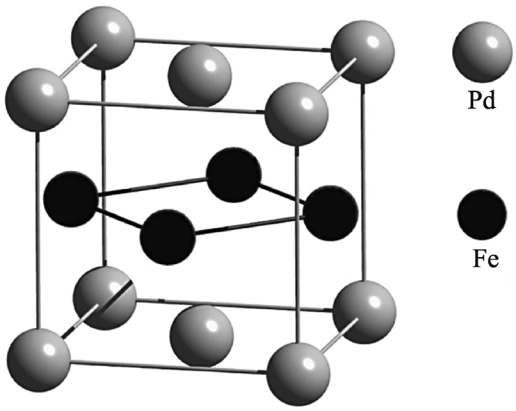

Fig. 2. Model of the location of atoms in the ordered structure of the $L1_0$ (or CuAuI) type with the layer-by-layer ordering of atoms of different types.

Changes in the polycrystalline reflections corresponding to Pd start to be observed in the electron diffraction pattern at a temperature of 400°C. They begin to increase in diameter. This indicates the change in the crystal lattice parameter without the change in its type, i.e., the formation of the Pd–Fe solid solutions. The change in the corresponding interplanar distances is ≈0.01–0.02 Å. For comparison, we note that the fcc lattice parameter is $a = 3.89$ Å in Pd, $a = 3.85$ Å in $Pd_{75}Fe_{25}$, and $a = 3.81$ Å in $Pd_{50}Fe_{50}$ and the atomic interplanar distance is $d(111) = 2.246$ Å in Pd, $d(111) = 2.24$ Å in $Pd_{75}Fe_{25}$, and $d(111) = 2.198$ Å in $Pd_{50}Fe_{50}$.

The diffraction reflections corresponding to the α-Fe and Pd phases are no longer observed in the electron diffraction pattern at a temperature of 480°C. This indicates that α-Fe and Pd reacted completely, forming the Fe–Pd disordered solid solution. In addition, four spot reflections $d \approx 2.7$ Å with the intensity <1% corresponding to the ordered FePd phase with the tetragonal structure (space group $P4/mmm$ with the lattice parameters $a = 3.852$ Å, $c = 3.723$ Å (PDF4+ card 03-065-9971)) appeared in the electron diffraction pattern at 480°C. This is the ordered structure of the $L1_0$ (or CuAuI) type with the layer-by-layer ordering of atoms of different types (see Fig. 2). The geometrical location of the observed diffraction reflections $L1_0$–FePd, $d(110) = 2.72$ Å indicates the orientation relation $L1_0$–FePd (001)[110] || α-Fe(001)[001].

During the further heating, the intensity of the diffraction reflections $L1_0$–FePd $d(110)$ increases gradually. Four spot reflections $d = 2.7$ Å with the intensity ~1% corresponding to $L1_0$–FePd $d(001) = 3.72$ Å

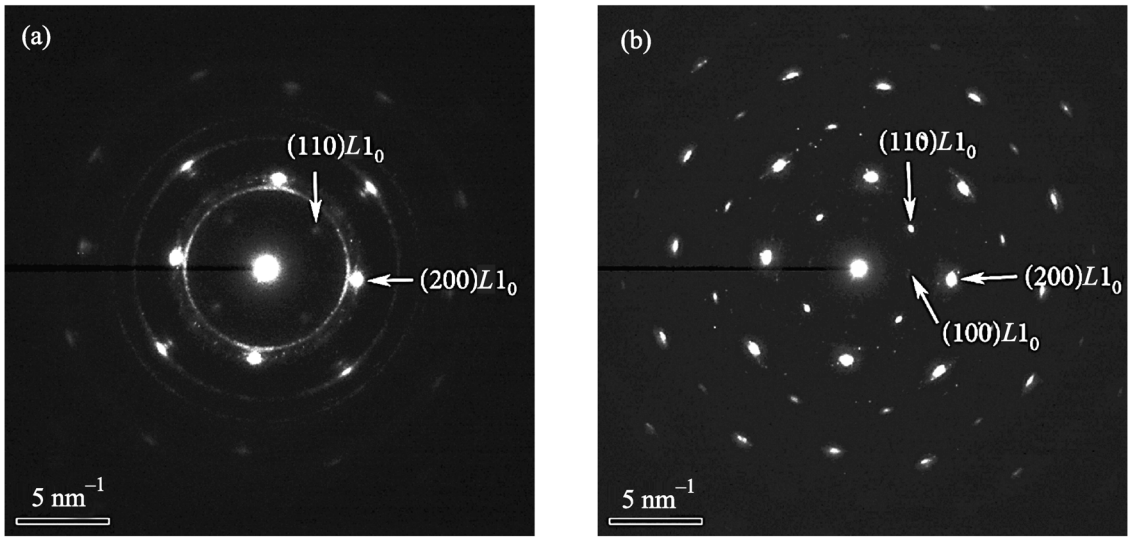

Fig. 3. Electron diffraction patterns of the Pd/α-Fe(001) film at a temperature of (a) 640 and (b) 700°C after annealing for 25 min.

appeared in the electron diffraction pattern at a temperature of 517°C.

Figure 3a shows the electron diffraction pattern obtained from the Pd/α-Fe(001) film at heating to 640°C. The analysis of the diffraction reflections indicates that the disordered FePd phase in the polycrystalline state (ring-type reflections) in the film is also present in addition to the ordered $L1_0$–FePd phase mainly being in the single-crystal state (spot-type diffraction reflections). In the process of annealing at 700°C, the intensity of reflections corresponding to the ordered $L1_0$ phase with the orientation (001) increases gradually. In addition, the transition from the polycrystalline $L1_0$ phase to the single-crystal phase takes place. After annealing for 25 min at 700°C (Fig. 3b), about 90% of the film volume is the single-crystal $L1_0$ phase with the orientation (001), and the rest is the polycrystalline $L1_0$ phase. The transmission electron microscopy image of the film after cooling to room temperature is shown in Fig. 4. Its analysis indicates that the average size of the crystal grains is 60 ± 10 nm. The analysis of the element composition of the films after annealing at 700°C and cooling to room temperature reveals the presence of only Fe and Pd (content of Pd is 50.2 ± 0.5 at %, content of Fe is 49.8 ± 0.5 at %). No oxygen was observed in the films.

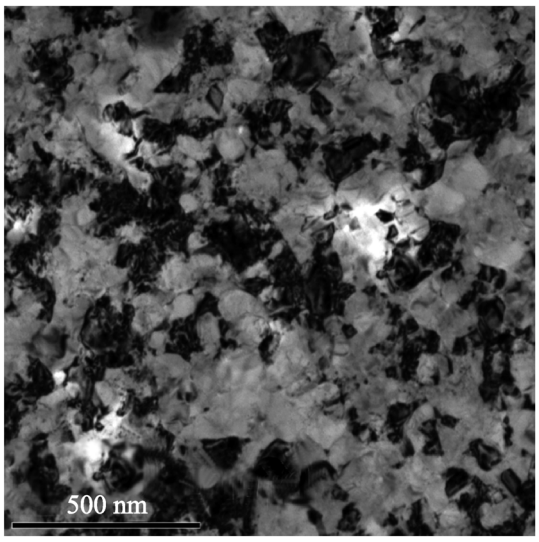

Fig. 4. Transmission electron microscopy image of the film Pd/α-Fe(001) after annealing for 25 min at 700°C and cooling to room temperature.

In order to analyze the temperature stability of the $L1_0$–FePd phase formed in the studied films, we performed the in situ electron diffraction studies of the change in the phase composition of the films in the process of heating from room temperature to 850°C. Heating was performed at a rate of 8°C/min. The intensity of the reflections of the $L1_0$-phase starts to decrease at 725°C. At a temperature of 740°C, the reflections of the $L1_0$-phase disappear, which indicates the complete transition of the ordered $L1_0$–FePd phase to the disordered FePd phase. It should be noted that, according to the phase equilibrium diagram [11], a palladium content of 52.5 at % corresponds to the phase transition temperature of the ordered $L1_0$–FePd phase to the disordered FePd phase of 740°C. For the Fe–Pd system with a palladium content of 50.2 at %, the order–disorder phase transition temperature should be 705°C [11]. Thus, the order–disorder phase transition temperature is shifted from the equilibrium value by 35°C toward higher temperature. The observed effect can be explained by the higher

concentration of palladium atoms at the boundaries of the Fe–Pd crystal grains due to the grain-boundary adsorption [18]. A similar effect was observed in zinc oxide films doped with manganese, cobalt, and iron [19] and in Fe–C alloys with the carbon concentration from 0.05 to 1.7 wt % [20]. In the case of manganese-doped zinc films, it was shown that the crystal zinc oxide nanograins are completely surrounded by the amorphous manganese-enriched region [19]. The ratio of the area of the surface of the boundaries of the crystal grains to the volume in the studied Fe–Pd films after annealing at 700°C, when the average grain size is 60 ± 10 nm (see Fig. 4) and the film thickness is 60 nm, is estimated as $\sim 10^7$–10^8 m^2/m^3.

Thus, the performed in situ experiments imply the following sequence of solid-state reactions in the thin-film system Pd/α-Fe(001).

1. The growth of the phase $Fe_3O_4(001)$ starts at 305°C owing to the interaction between Fe and oxygen adsorbed on the film surface. The growth of the $Fe_3O_4(001)$ phase with the orientation relation $Fe_3O_4(001)$ [110] ‖ α-Fe(001)[001] continues to 535°C. Then, it decreases. The thermal decomposition of Fe_3O_4 and the removal of the adsorbed oxygen from the Fe film surface take place at 550°C.

2. At 400°C, the solid-state reaction starts at the interface between the Fe and Pd layers. As a result, the atomically disordered Fe–Pd phase is formed.

3. The ordered single-crystal $L1_0$–FePd phase is formed at a temperature of 480°C. Its growth occurs with the orientation relation $L1_0$–FePd (001)[110] ‖ α-Fe(001)[001]. In addition, the complete mixing of the Fe and Pd layers takes place at a temperature of 480°C, and the thin-film system is a mixture of the ordered $L1_0$–FePd phase and disordered FePd phase.

4. Atomic ordering takes place in the process of annealing at 700°C. In 25 min, the single-crystal $L1_0$–FePd phase with the (001) orientation constitutes about 90% of the volume of the film and the rest is the polycrystalline $L1_0$–FePd phase.

5. The order–disorder phase transition starts at 725°C. At a temperature of 740°C, the transition of the ordered $L1_0$–FePd phase to the disordered FePd phase takes place over the whole film volume. The observed order–disorder phase transition temperature is shifted from the equilibrium value by 35°C toward higher temperatures. This effect can be assumingly attributed to the higher concentration of the palladium atoms at the boundaries of the Fe–Pd crystal grains owing to the grain-boundary adsorption.

This work was supported in part by the Russian Foundation for Basic Research (project no. 14-03-00515a) and by the Ministry of Education and Science of the Russian Federation (state contract for the Siberian Federal University for 2014).

REFERENCES

1. D. Weller and M. F. Doerner, Ann. Rev. Mater. Sci. **30**, 611 (2000).
2. I. Kaitsu, R. Inamura, J. Toda, and T. Morita, FUJITSU Sci. Tech. J. **42**, 122 (2006).
3. T. J. Klemmer, C. Liu, N. Shukla, X. W. Wu, D. Weller, M. Tanase, D. E. Laughlin, and W. A. Soffa, J. Magn. Magn. Mater. **266**, 79 (2003).
4. T. Schied, A. Lotnyk, C. Zamponi, L. Kienle, J. Buschbeck, M. Weisheit, B. Holzapfel, L. Schultz, and S. Fahler, J. Appl. Phys. **108**, 033902 (2010).
5. M. Ohtake, S. Ouchi, F. Kirino, and M. Futamoto, J. Appl. Phys. **111**, 07A708 (2012).
6. A. Kovacs, K. Sato, and Y. Hirotsu, J. Appl. Phys. **102**, 123512 (2007).
7. Y. Endo, Y. Yamanaka, Y. Kawamura, and M. Yamamoto, Jpn. J. Appl. Phys. **44**, 3009 (2005).
8. N. I. Vlasova, A. G. Popov, N. N. Shchegoleva, V. S. Gaviko, L. A. Stashkova, G. S. Kandaurova, and D. V. Gunderov, Acta Mater. **61**, 2560 (2013).
9. V. G. Myagkov, V. S. Zhigalov, L. E. Bykova, L. A. Soloviev, and G. N. Bondarenko, JETP Lett. **91**, 481 (2010).
10. V. G. Myagkov, V. S. Zhigalov, B. A. Belyaev, L. E. Bykova, L. A. Solovyov, and G. N. Bondarenko, J. Magn. Magn. Mater. **324**, 1571 (2012).
11. *Binary Alloy Phase Diagrams*, Ed. by T. B. Massalski, H. Okamoto, P. R. Subramanian, and L. Kacprzak, 2nd ed. (ASM Int., Materials Park, Ohio, 1990).
12. E. T. Moiseenko, R. R. Altunin, and S. M. Zharkov, Bull. Russ. Acad. Sci.: Phys. **76**, 1149 (2012).
13. G. S. Patrin, Ch.-G. Lee, I. A. Turpanov, S. M. Zharkov, D. A. Velikanov, V. K. Maltsev, L. A. Li, and V. V. Lantsev, J. Magn. Magn. Mater. **306**, 218 (2006).
14. N. V. Volkov, A. S. Tarasov, E. V. Eremin, S. N. Varnakov, S. G. Ovchinnikov, and S. M. Zharkov, J. Appl. Phys. **109**, 123924 (2011).
15. *Powder Diffraction File (PDF 4+, 2012), Inorganic Phases* (International Center for Diffraction Data, Swarthmore, PA, USA).
16. P. Villars and K. Cenzual, *Pearson's Crystal Data: Crystal Structure Database for Inorganic Compounds* (ASM International, Materials Park, Ohio, USA, 2011–2012), CD-ROM.
17. R. Mahesh, D. Sander, S. M. Zharkov, and J. Kirschner, Phys. Rev. B **68**, 045416 (2003).
18. B. B. Straumal, *Grain Boundary Phase Transitions* (Nauka, Moscow, 2003) [in Russian].
19. B. B. Straumal, S. G. Protasova, A. A. Mazilkin, et al., JETP Lett. **97**, 367 (2013).
20. B. B. Straumal, A. A. Mazilkin, S. G. Protasova, S. V. Dobatkin, A. O. Rodin, B. Baretzky, D. Goll, and G. Schutz, Mater. Sci. Eng. A **503**, 185 (2009).

Translated by L. Mosina